Pseudo-Hall Effect and Anisotropic Magnetoresistance in a Micronscale $Ni_{80}Fe_{20}$ Device

C.C. Yao, D.G. Hasko, W.Y. Lee, A. Hirohata, Y.B. Xu, and J.A.C. Bland
Cavendish Laboratory, University of Cambridge, Cambridge CB3 0HE, UK

Abstract — **The pseudo-Hall effect (PHE) and anisotropic magnetoresistance (AMR) in a micronscale $Ni_{80}Fe_{20}$ six-terminal device, fabricated by optical lithography and wet chemical etching from a high quality UHV grown 30 Å Au/300 Å $Ni_{80}Fe_{20}$ film, have been studied. The magnetisation reversal in different parts of the device has been measured using magneto-optical Kerr effect (MOKE). The device gives a 50% change in PHE voltage with an ultrahigh sensitivity of 7.3%Oe^{-1} at room temperature. The correlation between the magnetisation, magneto-transport properties, lateral shape of the device and directions of the external applied field is discussed based on extensive MOKE, AMR and PHE results.**

Index Terms — **pseudo-Hall effect, magnetoresistance, magnetisation reversal, MOKE**

I. Introduction

It is well known that many ferromagnetic materials and alloys show the anisotropic magnetoresistance (AMR) and the pseudo-Hall effect (PHE) [1-3], which are manifested in the dependence of the resistivity on the angle between the current and magnetisation direction. Recently, a new type of active device [4] and sensitive low-field magnetic sensors [5] have been developed and fabricated, based on the PHE. The advantage of magnetoresistive sensors, based on the PHE rather than on the AMR, is that temperature drift can be strongly reduced, which is the main factor limiting the low field performance of magnetoresistive sensors.

Owing to the shape-dependent demagnetising field, the magnetisation reversal and magneto-transport properties of micronscale structures are quite different from those of bulk ferromagnets [6]. The ability to control magneto-transport of small magnetic structures is becoming increasingly important in technological applications as novel magnetoelectronic devices are miniaturised. In this work, we have studied the PHE and AMR in a specially designed micronscale $Ni_{80}Fe_{20}$ six-terminal device, in which the longitudinal MR, transverse MR and angular dependent PHE voltage can be measured. In order to fully understand the AMR and PHE results, the magnetisation reversal in different parts of the device have been measured using magneto-optical Kerr effect (MOKE). The correlation between the magnetisation and the magneto-transport properties has been discussed based on the extensive MOKE, AMR and PHE results.

II. Experiments

The micronscale six-terminal Permalloy device consists of a long horizontal wire and two vertical wires (see Fig. 1). The width of the vertical wires is 10 μm and the length is 200 μm. The width and length of the horizontal wires are 20 μm and 600 μm, respectively. The separation between the centres of the vertical wires is 100 μm. The device was fabricated by optical lithography and a pattern transfer technique based on pure wet chemical etching. An ultrahigh vacuum (UHV) system with a base pressure of 3×10^{-10} mbar was used to prepare continuous film structures of the form 30 Å Au/300 Å $Ni_{80}Fe_{20}$/GaAs(001). The insulating GaAs substrate was thoroughly cleaned in acetone and rinsed in isopropyl alcohol (IPA) before being load into the chamber, then it was heated to 600 °C to remove the oxide layer. The $Ni_{80}Fe_{20}$ layers were deposited at a rate of 1.2 Å/min. The pressure during growth was 5×10^{-10} mbar while the substrate was held at 30 °C. The film was annealed at 150 °C for 30 minutes to remove the uniaxial anisotropy induced during growth. The film was then capped with 30 Å of Au. After patterning the film by optical lithography, the pattern was transferred to the Au layer by wet chemical etching with a very weak solution of KI_2 for about 1 minute, using the patterned optical resist as a mask. The pattern is further transferred to the underlying $Ni_{80}Fe_{20}$ using wet chemical etching with a solution of $HCL:HNO_3:H_2O$ (1:25:200) [7]. This is made possible because of the high etch selectively between Au and $Ni_{80}Fe_{20}$. Finally, the remaining optical resist was completely stripped off in Acetone.

For a better understanding of the magnetisation reversal phenomena, the microscopic hysteresis loops in four different positions of the device have been measured by MOKE. Microscopic MOKE magnetometry measurements were carried out at room temperature using a stabilised HeNe laser source, with the in-plane magnetic field applied (H) parallel and perpendicular to the long axis of the device. An objective len (×50, Numerical Aperture: 0.85) was used to focus the probing laser beam (~ 1μm spot size) on the device. For the AMR and PHE measurements, electrical contacts to the six terminals of the sample were made using standard optical lithography, metallisation, a lift-off of 25 nm Cr/300 nm Au. The magneto-transport measurements were made at room temperature with the field applied in the plane of the device.

III. Results and Discussion

Fig.1 shows the device geometry and the microscopic hysteresis loops measured in four different positions (α, β, γ, and δ) of the device by MOKE microscopy, with the in-plane field applied parallel (Figs. 1(a)-1(d)) and perpendicular (Figs. 1(e)-1(h)) to the long wire axis. Position γ and position δ are the centre of the cross junction and device, respectively. As expected, owing to shape anisotropy, different hysteresis loops were obtained in different positions

Manuscript received May 28, 1999
C. C. Yao, 44 1223 337556, fax 44 1223 337706, ccy20@cam.ac.uk

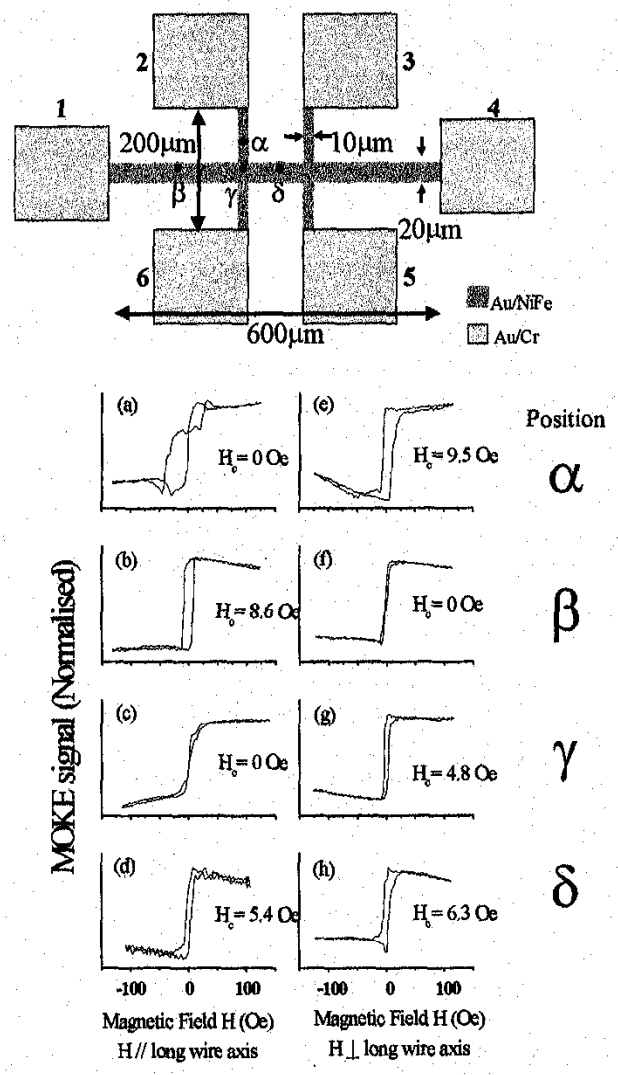

Fig. 1.Device geometry and microscopic MOKE hysteresis loops measured in four different positions (α, β, γ and δ) of the device by scanning Kerr microscopy with the field applied parallel and perpendicular to the long axis of the device.

of the device. Figs. 1(a), 1(c) and 1(f) show a zero (H_c=0) coercive force and Fig. 1(e) shows the largest coercive force among others.

Several interesting points related to the magnetisation reversal processes in different parts of the device are observed. First, comparing the microscopic MOKE hysteresis loops in Fig. 1(c) and Fig. 1(g), both measured in position γ, we observe that vertical direction is the easy axis direction of shape anisotropy in the cross junction centre as a non-zero coercive field H_c is shown in Fig. 1(g). This is in agreement with results from magnetic force microscopy (MFM) images as well as from analytical calculation [8]. Comparing the hysteresis loops in Fig. 1(a) and Fig. 1(f), measured in position α and β, respectively, a higher from terminal 1 and terminal 4. The most striking result is that in Fig. 3(b), the PHE response shows a 50% change and saturation field is seen in Fig. 1(a). Both of them are hard MOKE loops with zero coercive field. For a hard MOKE loop, the magnetisation reversal process is mainly by spin rotation. The difference between the two saturation results from the dependence of the saturation field on the demagnetising field [9], which is inversely proportional to the width of the wires. A higher coercive field is observed in Fig. 1(e) compared with Fig. 1(b). Both are easy MOKE loops with rectangular shapes. The increase in the coercive field with reduced width is in qualitative agreement with the results of earlier work [7]. This behaviour can be attributed to the fact that that domain wall propagation mechanism involved in the magnetisation reversal is modified as the width of the wires is reduced. Last, a non-zero coercive force is observed in Fig. 1(h), implying that domain wall motion occurs in the centre of the device with the field applied perpendicular to the long wire axis, and the magnetisation reversal process in the device centre is strongly influenced by the presence of the nearly vertical wires.

For magneto-transport measurements, a constant current (I = 1mA) is driven from terminal 1 to terminal 4 and the voltage (V_{ij}) is measured between terminals i and j as a function of an in-plane magnetic field. Fig. 2. shows, in (a) and (c), the AMR response curves (V_{23}/I) and, in (b) and (d), the PHE response curves (V_{35}/I), for the field applied parallel and perpendicular to the long wire axis of the device, respectively. It should be noted that V_{23}/I is the ordinary AMR signal and V_{35}/I is the PHE signal.

Fig. 2(a) shows a typical longitudinal MR curve for wires [7], in which the sharp resistance minimum corresponds to the switching of the magnetisation in the wires, which is consistent with the MOKE hysteresis loop in Fig. 1(d). In Fig. 2(c), an negative transverse MR behaviour is seen. Unlike the typical transverse MR curve, two clearly separated peaks in the MR curve are observed and which occur at the field corresponding to the coercive field in Fig. 1(h), implying that the reversal process is not purely by spin rotation, and the domain wall motion, induced by the magnetisation reversal in the vertical wires, occurs at the centre of the device.

Fig. 2(b) and 2(d) show the PHE response curves. For both curves, as the applied field H is increased from the negative maximum, the voltage clearly increases and then drops abruptly after H reverses. At low positive fields, the voltage reaches a minimum and increases, and then saturates at higher positive fields. It is interesting to note that the PHE signal is proportional to $\cos^2(\theta-45^0)$ and the AMR signal is proportional to $\cos^2\theta$, where θ is the angle between the localised magnetisation and the current density. Therefore, comparing the AMR and PHE response curves, we expect to a see a 45^0 phase shift in θ.

Figs. 3(a) and 3(b) show the PHE response curves with fields applied at 45^0 and 135^0 with respect to the long wire axis of the device, respectively. The voltage is measured between terminals 3 and 5 when current flow from terminal 1 and terminal 4. The most striking result is that in Fig. 3(b), the PHE response shows a 50% change and an ultrahigh sensitivity of 7.3% Oe^{-1} over 6 Oe with a magnetic field of less then 20 Oe. The absolute value of the

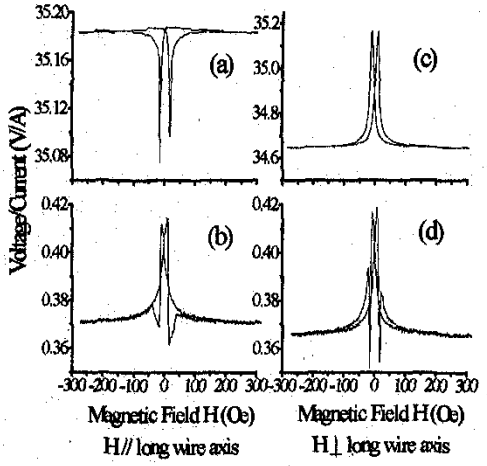

Fig. 2. (a), (c) AMR response curves (V_{13}/I) and (b), (d) PHE response curves (V_{35}/I) for the field applied parallel and perpendicular to the long axis of the device, respectively. In V_{ij}, the voltage is measured between terminals i and j when current flows from terminal 1 to terminal 4.

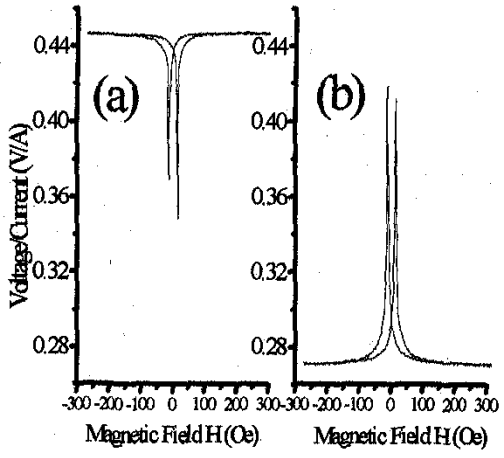

Fig. 3. PHE response curves with fields applied at (a) 45° (b) 135° with respect to the long wire axis of the device. The voltage is measured between terminals 3 and 5 when current flows from terminal 1 to terminal 4.

PHE response is about 150 mV/A. This result is reproducible and stable in all devices fabricated. Although higher relative changes in the PHE voltage have been reported [10-12], this is the highest reported sensitivity and absolute value of the PHE output change in a homogenous $Ni_{80}Fe_{20}$ device. Such high sensitivity is not expected to be observed in magnetoresistive sensors based on PHE or AMR with regular rectangular shapes. It is believed that higher PHE change and sensitivity can be obtained by systematic study of the lateral shape effect to the magnetic properties of *micronscale devices*.

IV. Conclusions

In conclusion, the magnetisation reversal processes and magneto-transport behaviour in a homogenous micronscale $Ni_{80}Fe_{20}$ six-terminal device have been studied using MOKE, MR and PHE. The correlation between the magnetisation and magneto-transport properties has been discussed based on extensive MOKE, AMR and PHE results. Our study not only has implications for the understanding of fundamental *magnetism in micronscale structures, but also could provide* a way of improving the performance of practical magnetoresistive devices.

Acknowledgement

The authors would like to thank Prof. H. Ahmed for providing the fabrication facilities for this work. C.C.Y. acknowledges scholarship from the Croucher Foundation.

References

[1] T.R. McGuire and R.I. Potter, "Anisotropic magnetoresistance in ferromagnetic 3d Allos," IEEE Trans. Mag. **11**, 1018 (1975).

[2] D.A. Thompson, L.T. Romankiw, and A.F. Mayadas, "Thin film magnetoresistance in memory, storage, and related applications," IEEE Trans. Mag. **11**, 1039 (1975).

[3] P. Ciureanu: "Magnetoresistive Sensors" in *Thin Film Resistive Sensors*, edited by P. Ciureanu and S. Middelhoek (institue of Physics Publishing, Bristol, 1992), P.253.

[4] K. Kakuno, "New type of active device based on galvanomagnetic effect," J. Appl. Phys. **81**, 8105 (1997).

[5] A. Schuhl, F. Nguyen Van Dau, and J.R. Childress, "Low-field magnetic sensors based on the planar Hall effect," Appl. Phys. Lett. **66**, 2751 (1995).

[6] K. Hong and N. Giordano, "Approach to mesoscopic measurements," Phys. Rev. B **51**, 9855 (1995).

[7] A.O. Adeyeye, J.A.C Bland, C. Daboo, D.G. Hasko and H. Ahmed, "Size dependence of the magnetoresistance in submicron FeNi wires," J. Appl. Phys. **79**, 6120 (1996).

[8] C.C. Yao, PhD Thesis, University of Cambridge (1999).

[9] B.B. Pant, "Effect of interstrip gap on the sensitivity of high sensitivity magnetoresistive transducers," J. App. Phys. **79**, 6123 (1996).

[10] Y.Q. Jia, L. Kong, R.C. Shi, and S.Y. Chu, "Effects of sample size and field orientation on pseudo-Hall voltage in micronscale nickel thin-film squares," J. Appl. Phys. **81**, 5475 (1997).

[11] B. Zhao, X. Yan, and A.B. Pakhomov, "Anisotropic magnetoresistance and planar Hall effect effect in magnetic metal-insulator composite films," J. Appl. Phys. **81**, 5527 (1997).

[12] C. Prados, D. Garcia, F. Lesmes, J.J. Freijo, and A. Hernando "Extraodinary anisotropic magnetoresistance effect under 35 Oe field at room temperature in Co/Ni multilayers," Appl. Phys. Lett. **67**, 718 (1997).